

Performance Analysis of a Sliding Mode Control for Distributed Generations

Gazi Islam*, Ahmed Al-Durra*, Cedric Caruna*, S. M. Muyeen*, and Junji Tamura**

* Department of Electrical Engineering, The Petroleum Institute, UAE

** Department of Electrical Engineering, Kitami Institute of Technology, Japan

Abstract—This paper presents the performance of a sliding mode based hybrid controller for three phase voltage source inverter. The main objective of this analysis is to observe the effectiveness of the controller for fault ride through (FRT) capability improvement of the DC based distributed generations (DG). The performance of the conventional PI based cascaded controller is also presented for comparison purpose.

Index Terms— Current control, distributed power generation, power system faults, PSCAD.

I. INTRODUCTION

The main driving force for using renewable energy as distributed generation (DG) is its zero carbon emission. In addition to small residential systems, centralized MW class large renewable energy conversion systems are also growing very fast over the last decade. Apart from the environmental benefits, grid connected distributed generation systems have a number of impacts on the existing power systems either in a positive or negative ways. Installation of distributed generations can reduce the transmission line loading and losses incurred for this. This is due to the fact that less amount of power needs to be transferred through the transmission lines from the conventional power plants as some load demand will be served by the DGs at the distribution level. It can also delay the up-gradation of transformers and transmission lines, and reduce the frequency of their maintenance works [1]. However, transmissions lines are, in general, highly efficient and major power losses occur in the distribution networks. Increase of power flow in distribution network can increase the overall power loss of the system. Therefore, addition of DGs may increase the overall line losses unless their locations are chosen carefully depending on the load conditions [2]. They can provide a good support during peak power demand and thus electricity generation from DGs can also be cost effective. The installation of DGs can improve the voltage profile at the point of common coupling (PCC) and oscillatory stability of the power systems [3], [4].

However, the major concern of using grid interfaced distributed system is its intermittency. This reduces the reliability of the overall system. Alternatively, the penetration level of PV plants has to be sufficiently low to maintain the same reliability of operations. Besides, integration of DGs can introduce power quality problems like flicker, voltage dips, harmonic distortion, etc.

The impact of distributed generation to the power system is fast becoming significant due to the increase of grid connected applications of alternative energy sources. Because of higher penetration to the grid, the requirement

of providing dynamic grid support by these renewable energy sources is becoming important. For example, grid connected PV plants must remain connected to the power system during the fault conditions, as per recent German grid codes [5], [6]. This means the DGs will ride through the fault. Fault ride through (FRT) requirement has already been implemented in many countries for wind energy systems. This means that the plants must be able to

- remain connected to the network during grid faults,
- provide dynamic voltage support by delivering reactive power,
- reduce the reactive power delivery fast to the steady-state value after the fault is cleared.

The limiting curves for type 2 generators (plants other than synchronous generators) are shown in Fig. 1 [5]. When the terminal voltage drops down to 0 pu, the plant can only be disconnected from the network if the duration of this voltage level persists for more than 150 ms. The recovery of the voltage has to be fast enough during the post fault condition that the terminal voltage recovers 90% of its nominal value within 1.5s. Hence, for the fault ride through requirement of the grid connected DG system the major challenge is its grid side inverter control; the inverter must have fast transient response to regulate the DC link voltage, under and overvoltage protection, and fast terminal voltage recovery capability if there is any fault in the system.

This paper presents a comparative analysis of the performance of a sliding mode based hybrid controller with that of the conventional PI controller based inverter connected to DC based distributed generations with a focus on the fault ride through (FRT).

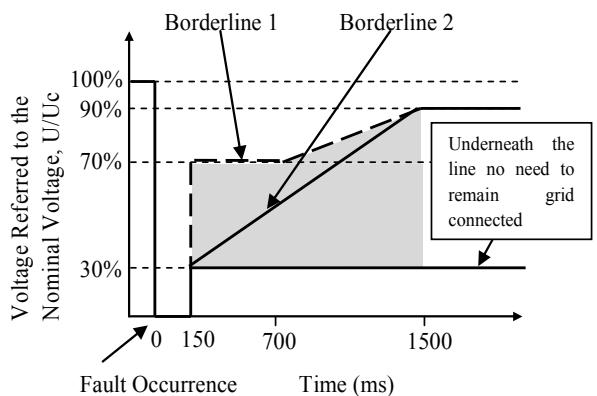


Fig. 1. Limiting curves of the voltage of a type-2 generator at the point of connection [5].

II. GRID INTEGRATION OF DG

The application of power conditioning units (PCU) can be classified into two categories. Input side converters are generally used to control the DG to operate in the maximum power point. Grid side converters, on the other hand, generally control the real and reactive power delivery to the grid by regulating DC link voltage and grid side terminal voltage respectively. Figure 2 shows the DC based grid integrated DG system which has been used for this study. In this system a 5 MW plant is connected to the DC side of the three phase voltage source inverter. The AC side of the inverter is connected to the double circuit transmission line via a step up transformer. The parameters for the system are given in Table I.

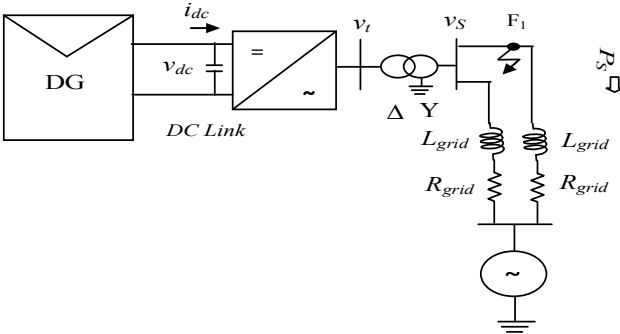


Fig. 2. System structure of grid integrated DG

TABLE II
LINE PARAMETERS

V_{dc}	1.2 kV
Transformer voltage ratio (Δ -Y)	0.763 kV/ 22 KV
R_{grid} (for each line)	9.68 Ω
L_{grid} (for each line)	0.18487 H

III. CONTROL OF VOLTAGE SOURCE INVERTER

The control of voltage source inverter is generally twofold. The outer loops control the real and reactive powers by controlling DC link voltage and grid side terminal voltage respectively, and generate the reference currents for the inner loops. The inner loops regulate the grid side currents to track the reference values so that required real and reactive powers are delivered successfully to the grid.

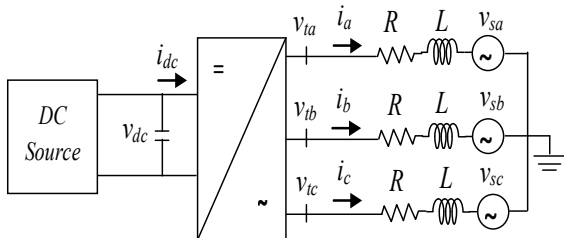


Fig. 3. System structure of grid integrated DG

A. Outer Loop Control

Figure 3 shows the three phase view of the grid

connected inverter. Let us suppose, the grid side d and q axis voltages and currents are v_{sd} , i_d and v_{sq} , i_q respectively. The equations for grid side real and reactive power in space phasor form are given by:

$$P_s = \frac{3}{2}(v_{sd}i_d + v_{sq}i_q) \quad (1)$$

$$Q_s = \frac{3}{2}(-v_{sd}i_q + v_{sq}i_d) \quad (2)$$

Using phase lock loop (PLL), v_{sq} is set to zero. Hence eqns. (1) and (2) reduce to:

$$P_s = \frac{3}{2}v_{sd}i_d \quad (3)$$

$$Q_s = -\frac{3}{2}v_{sd}i_q \quad (4)$$

Let us suppose transformer resistance and inductance are R and L respectively. R is very small compare to L . Hence, power loss across R is generally ignored. Ignoring the switching losses, the following relationship can be found during steady state:

$$P_{dc} \approx P_t \approx P_s = P \quad (5)$$

Again from dc side:

$$P_{dc} = v_{dc}i_{dc} \quad (6)$$

Therefore, from eqns. (3), (5), and (6), it can be stated that reference current for d-axis (i_d^*) can be obtained by controlling the DC link voltage. Reactive power transfer Q_s is directly proportional to the terminal voltage V_s . Hence from eqn. (4), the reference current for q-axis (i_q^*) can be found by regulating terminal voltage V_s .

1. Conventional PI based cascaded control

As mentioned above the i_d^* and i_q^* can be generated by regulating DC link voltage and grid side terminal voltage. Therefore, in conventional PI based inverter control, the following equations are used for the outer control loops:

$$i_d^* = (K_{P_Vdc} + \frac{K_{I_Vdc}}{s})(v_{dc}^* - v_{dc}) \quad (7)$$

$$i_q^* = (K_{P_Vs} + \frac{K_{I_Vs}}{s})(v_s^* - v_s) \quad (8)$$

where K_{P_Vdc} , K_{I_Vdc} , and K_{P_Vs} , K_{I_Vs} are the gains of the PI controllers; v_{dc}^* and v_s^* are reference DC link voltage and reference grid side voltage respectively

2. Sliding mode based hybrid control

For the sliding mode based hybrid control, the following first-order sliding surfaces are considered for the outer control loops [7]:

$$S_{Vdc} = e_{vdc} + K_{Vdc} \frac{de_{vdc}}{dt} \quad (9)$$

$$S_{VS} = e_{vs} + K_{VS} \frac{de_{vs}}{dt} \quad (10)$$

where $e_{Vdc} = v_{dc}^* - v_{dc}$ and $e_{VS} = |v_s^*| - |v_s|$. K_{Vdc} , K_{VS} are sliding surface coefficients. Reference d and q axis currents are generated using the following two equations [8]:

$$i_d^* = e_{Vdc} \left(K_{P_Vdc} + \frac{K_{I_Vdc}}{s} \right) + |S_{Vdc}| \cdot K_{S_Vdc} \cdot \text{sgn}(S_{Vdc}) \quad (11)$$

$$i_q^* = e_{VS} \left(K_{P_VS} + \frac{K_{I_VS}}{s} \right) + |S_{VS}| \cdot K_{S_VS} \cdot \text{sgn}(S_{VS}) \quad (12)$$

where K_{P_Vdc} , K_{I_Vdc} , K_{P_VS} , K_{I_VS} , K_{S_Vdc} , and K_{S_VS} are the controller gains. The sliding mode controllers help to reject large voltage disturbances. The sliding surface magnitudes are also used as adaptive gains. They provide large gains during grid faults fast for voltage recovery. They also reduce the chattering problem because of the smaller gains during the steady state. The PI controllers control the settling time and overshoot to some extent.

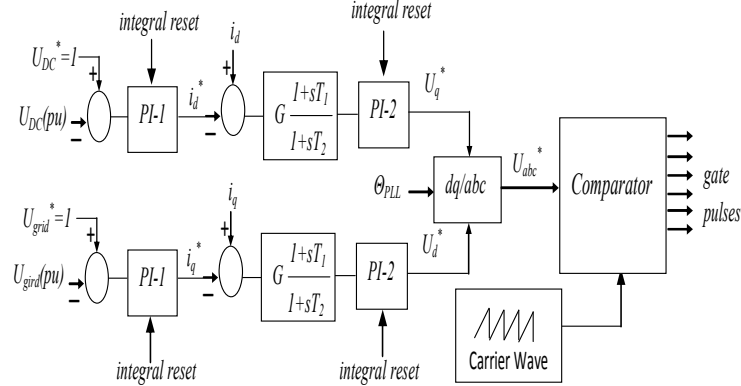


Fig. 4. PI based cascaded control

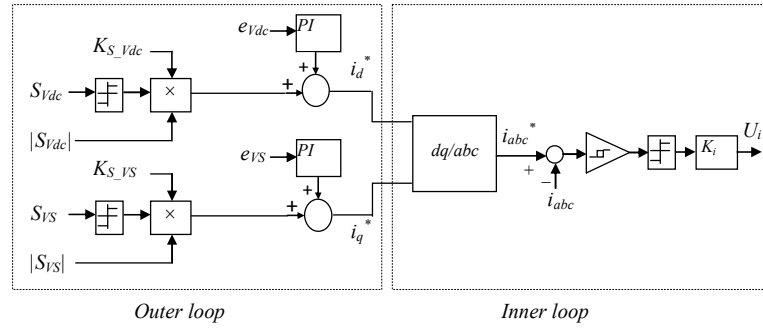


Fig. 5. Sliding mode based hybrid control

B. Inner Loop Control

1. Conventional PI based cascaded control

The block diagram of PI based conventional controller

for three phase voltage source inverter is shown in Fig. 4 [9]. The outer loops generate the reference currents using eqns. (7) and (8). In the inner loop the error signals of the d and q axis currents are progressed through PI controller to generate the reference voltage in d-q axis. They are transformed from d-q axis to abc axis and are given to the comparator block to generate gate pulses for the IGBTs.

2. Sliding mode based hybrid control

The control block for sliding mode based hybrid control is shown in Fig. 5. The outer loops are designed based on eqns. (11) and (12). The inner loop control design is described below.

From Fig. 3 the following state space equations can be found:

$$L \frac{di_a}{dt} = -Ri_a + v_{ta} - v_{sa} \quad (13)$$

$$L \frac{di_b}{dt} = -Ri_b + v_{tb} - v_{sb} \quad (14)$$

$$L \frac{di_c}{dt} = -Ri_c + v_{tc} - v_{sc} \quad (15)$$

B. Inner Loop Control

1. Conventional PI based cascaded control

The block diagram of PI based conventional controller

Voltage drop across the resistance is very small and generally ignored. When the upper switch is conducting and the lower switch is off, for each leg the following

relationship can be obtained:

$$L \frac{di_i}{dt} = \frac{1}{2} v_{dc} - v_{si} > 0 \quad i = a, b, c \quad (16)$$

Similarly when the upper switch is off and lower switch is conducting:

$$L \frac{di_i}{dt} = -\frac{1}{2} v_{dc} - v_{si} < 0 \quad i = a, b, c \quad (17)$$

From eqn. (16) and (17) it is clear that the current slope is positive when $v_t = v_{dc}/2$ and negative for $v_t = -v_{dc}/2$. Therefore, the following sliding mode control laws are considered:

$$v_{ti} = K_i \text{sign}(S_i) \frac{v_{dc}}{2} \quad i = a, b, c \quad (24)$$

where $S_i = i_i^* - i_i$; this implies:

$$L \frac{di_i}{dt} = K_i \text{sign}(S_i) \frac{v_{dc}}{2} - v_{si} > 0 \quad i = a, b, c \quad (25)$$

$$\dot{S}_i = \frac{di_i^*}{dt} - K_i \text{sign}(S_i) \frac{v_{dc}}{2L} + \frac{v_{si}}{L} \quad i = a, b, c \quad (26)$$

The reaching condition for the sliding surface is $S_i \dot{S}_i < 0$. Therefore, the value of K_i should be:

$$K_i > 2 \left[L \frac{di_i^*}{dt} + v_{si} \right] / v_{dc} \quad i = a, b, c \quad (27)$$

The switching laws are defined as follows:

$U_i > 0$; Upper switch is On and lower switch is Off
 $U_i < 0$; Upper switch is Off and lower switch is On

where $U_i = K_i \text{sign}(S_i)$. A hysteresis buffer is also used to limit the switching frequency and avoid the chattering problem.

IV. SIMULATION RESULTS

The comparative analysis of the conventional PI control and sliding mode based hybrid control for dynamic as well as transient performance is done in this study. The simulations are performed using PSCAD/EMTDC. The dynamic analysis of the controllers is shown in Fig. 6. In this figure the power generation from the DG has been varied with time. From the graph of the terminal voltage, it can be observed that it has oscillations during the power variations for the conventional PI controller. On the other hand, the terminal voltage variation is very less with the varied power generation for sliding mode based hybrid control. In case of DC link voltage there is a significant improvement in the dynamic performance for sliding mode based hybrid control.

The transient analysis is done to study the effectiveness of the sliding mode based hybrid controller for the fault ride through of the distributed generations and compare it with that of the PI controller. For transient analysis,

different symmetrical and unsymmetrical faults are considered at F1 location, shown in Fig. 2, in one of the double circuit transmission lines. All the faults are considered at 0.1 s, breakers opened at 0.25 s. Therefore, duration of the fault in the network is 0.15 s; this is the maximum time of fault for which the DG needs to remain connected to the grid. The fault is cleared at 0.3 s and the breakers reclosed at 0.8 s.

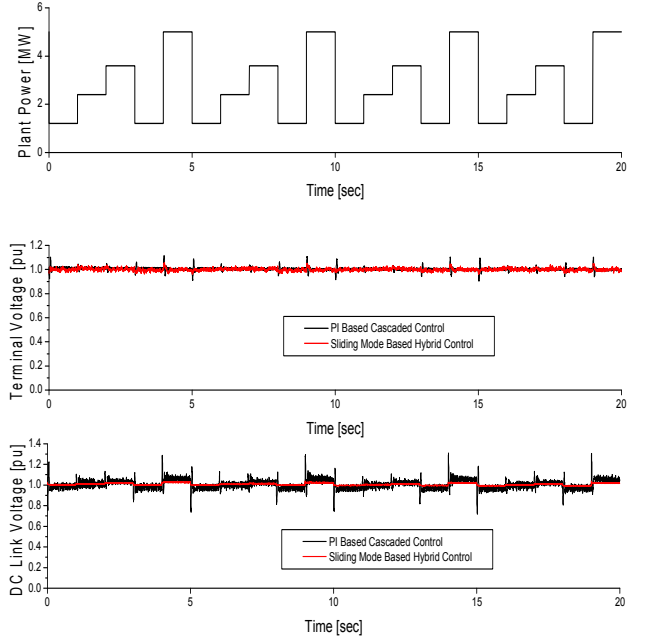


Fig. 6. Dynamic Performance

Figures 7 and 8 show the comparative transient performance of the two controllers for grid side terminal voltage and DC link voltage respectively for 3LG fault. Integral controller reset is considered during the faults for both control methods to avoid the voltage overshoots. The grid side voltage recovery after the breaker operation is very fast in case of both the controllers. But there are more oscillations in case PI controller.

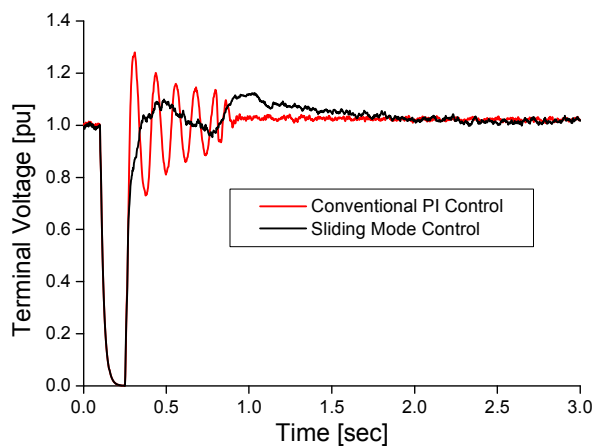


Fig. 7. Grid side terminal voltage (3LG fault)

For DC link voltage, much improved performance can be achieved for sliding mode based hybrid control compare to PI controller. The DC link voltage dip in case of PI controller may lead to the shutdown of the system, which does not comply with the requirements of fault ride through; also there is large voltage overshoot which can damage the devices unless any protection circuit is not used. Whereas the DC link voltage overshoot for sliding mode controller is less than 1.2 pu and it recovers to 1 pu immediately after the breaker operation to isolate the fault.

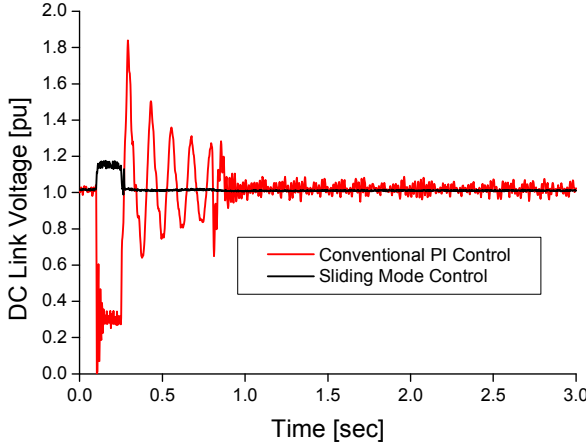


Fig. 8. DC link voltage (3LG fault)

The phase current (I_a) with its reference value (I_{a^*}) for sliding mode based hybrid controller are shown in Fig. 9. The figure shows the phase current for steady-state, during the fault and after the fault. It can be seen that the phase current can successfully track its reference value in all the conditions. Therefore, better responses for terminal voltage and DC link voltage, shown in Figs. 7 and 8, have been achieved.

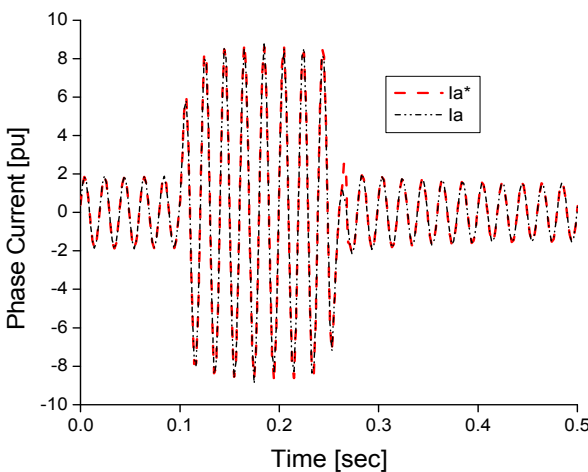


Fig. 9. Phase -a Current

Similarly, responses for grid side terminal voltage and DC link voltage for 2LG, 1LG, and LL faults for sliding mode based hybrid controller are shown in Figs. 10 and

11 respectively. For all types of fault, the system can recover the terminal voltage successfully and there are very little overshoots. The DC link voltage overshoots are

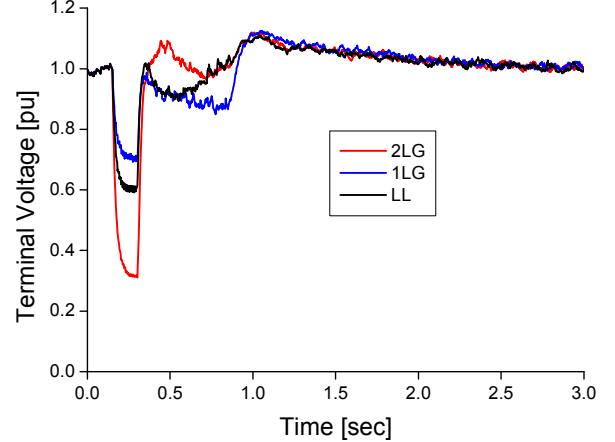


Fig. 10. Grid side terminal voltage

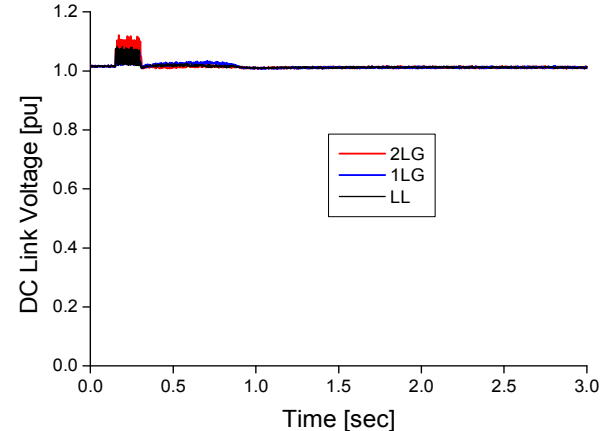


Fig. 11. DC link voltage

V. CONCLUSIONS

In this paper, a sliding mode based hybrid inverter control has been discussed. The performance of the controller is compared with that of a conventional PI controller. It has been found that the sliding mode based hybrid controller has much better current tracking capability, and gives improved terminal voltage and DC link voltage during grid faults. The dynamic performance of the controller is also better than that of the PI controller. Hence, it can be concluded that the sliding mode based hybrid controller gives improved dynamic as well as transient performance for grid connected DC based distributed generations.

REFERENCES

- [1] T. Hoff, and D. Shugar, "The value of grid-support photovoltaics in reducing distribution system losses," *IEEE Trans. Energy Conv.*, vol. 10, no. 3, pp. 569-576, Sep. 1995.

- [2] L. Freris, and D. Infield, *Renewable Energy in Power Systems*. West Sussex: John Wiley & Sons. Ltd, 2008, pp. 187.
- [3] W. Omran, M. Kazerani, and M. Salama, "A Study of the Impacts of Power Fluctuations Generated from Large PV Systems," *IEEE PES/IAS Conf. Sustainable Alternative Energy (SAE)*, Valencia, Sep. 2009.
- [4] R. Shah, N. Mithulananthan, A. Yome, and K. Lee, "Impact of Large-Scale PV Penetration on Power System Oscillatory Stability," *IEEE PES General Meeting*, Minneapolis, Jul. 2010.
- [5] "Technical guideline – generating plants connected to the medium-voltage network," *Bundesverband der Energie- und Wasserwirtschaft, BDEW*, Jun. 2008.
- [6] "Transmission code 2007 – network and system rules of the German transmission system operators," *Verband der Netzbetreiber (VDN)*, Aug. 2007.
- [7] Y. Mohamed, and E. El-Saadany, "A control scheme for PWM voltage-source distributed-generation inverters for fast load-voltage regulation and effective mitigation of unbalanced voltage disturbances," *IEEE Trans. Ind. Electron.*, vol. 55, no. 5, May 2008.
- [8] G. Islam, A. Al-Durra, S.M. Muyeen, and J. Tamura, "A Robust Control Scheme to Enhance the Stability of a Grid-connected Large Scale Photovoltaic System," accepted in *IEEE PES Transmission and Distribution Conference and Exposition*, Orlando, Florida, USA, May 2012.
- [9] G. Islam, A. Al-Durra, S.M. Muyeen, and J. Tamura, "Low Voltage Ride Through Capability Enhancement of Grid Connected Large Scale Photovoltaic System," in *Proc. IEEE Annu. Conf. Ind. Electron. Soc. (IECON'11)*, Melbourne, Australia, Nov. 2011.